Process Design of Bamboo Carbon Reinforced Polylactic Acid Composites *via* Twin-Screw Extrusion

Haoxiang Fang,[a,b,c] Kangjian Zhang,[c] Yuxuan Chen,[a,b] Linpeng Yu,[a,b] Ping Zhu,[a,b] Bin Xu,[c] and Genlin Tian [a,b,*]

** Corresponding author: tiangenlin@icbr.ac.cn (G. Tian)*

DOI: 10.15376/biores.21.2.3449-3468

GRAPHICAL ABSTRACT

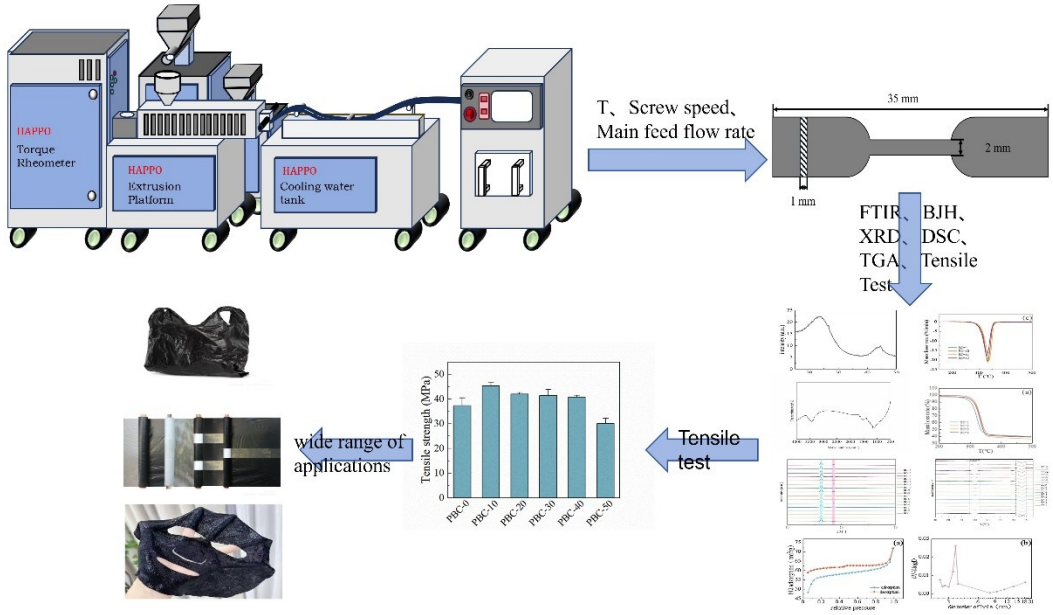

Process Design of Bamboo Carbon Reinforced Polylactic Acid Composites *via* Twin-Screw Extrusion

Haoxiang Fang,[a,b,c] Kangjian Zhang,[c] Yuxuan Chen,[a,b] Linpeng Yu,[a,b] Ping Zhu,[a,b] Bin Xu,[c] and Genlin Tian [a,b,*]

Bamboo carbon (BC) reinforced polylactic acid (PLA) composites play a significant role in optimizing the utilization of bamboo resources and advancing green, low-carbon, and circular development. To minimize production costs, a relatively high content of bamboo carbon (40 wt.%) was incorporated into the PLA matrix. However, for the high content of BC filler, the optimal process of balancing filler amount and interfacial properties is still unknown. In this study, a three-factor, four-level orthogonal experimental design was employed to investigate the effects of various processing parameters, initiated with twin-screw extrusion, on the crystalline structure, thermal properties, and mechanical performance of the composites. The optimal processing conditions for BC/PLA composites were determined to be a processing temperature of 195 °C, a screw speed of 120 rpm, and a feed rate of 15 g/min. Under these conditions, the tensile strength of the resulting composite reached 40.9 MPa. This study provides valuable insights for enhancing the performance of BC/PLA composites while promoting their large-scale application in sustainable materials engineering.

DOI: 10.15376/biores.21.2.3449-3468

Keywords: Bamboo carbon; Polylactic acid degradable; Composites; Process; Twin-screw extruder

Contact information: a: Institute of New Bamboo and Rattan Based Biomaterials, International Center for Bamboo and Rattan, Beijing 100102, China; b: Key Laboratory of National Forestry and Grassland Administration/Beijing for Bamboo & Rattan Science and Technology, Beijing 100102, China; c: School of Materials and Chemistry, Anhui Agricultural University, Hefei, Anhui 230036, China;
** Corresponding author: tiangenlin@icbr.ac.cn (G. Tian)*

INTRODUCTION

Polymer matrix composites have attracted extensive attention in recent decades because their properties can be effectively tailored through the selection of matrix materials, fillers, and processing methods (Alarifi 2023). Composite materials have overcome the performance limitations of traditional single-component materials and have created substantial value in various industrial applications (Anwer and Naguib 2016; Backes *et al.* 2019). In modern aerospace engineering, carbon fiber–reinforced ultra-high-temperature ceramic composites are considered ideal materials for manufacturing engines and hypersonic vehicles (Chaudhary *et al.* 2001; Binner *et al.* 2020). Glass fiber composites are widely used in automotive components such as doors and body panels to improve safety while significantly reducing vehicle weight (Dobrzański 2006; Cuadri and Martín-Alfonso 2018). Among various types of composites, thermoplastic polymer matrix composites, such as those based on polylactic acid (PLA) and polyolefins, have attracted significant attention due to their melt processability, recyclability, and suitability for extrusion-based

manufacturing (Friedrich and Almajid 2013; Douglas *et al.* 2015; Dubey *et al.* 2017; Ferdinand *et al.* 2023).

Scientists are increasingly focusing on the development of filler-modified polymer composites. Among various biodegradable polymers, PLA has emerged as one of the most extensively studied materials due to its eco-friendly and straightforward preparation process (Fu *et al.* 2008; Hietala and Oksman 2018; Ghorbani and Amirahmadi 2024). However, its inherent brittleness makes it susceptible to fracture under external impacts. Consequently, the modification of PLA to overcome this drawback has become a major research focus (Kuan *et al.* 2008; Ho *et al.* 2015). Numerous studies have investigated PLA-based composites incorporating inorganic fillers, plant fibers, and biomass carbon (Liu and Zhang 2011; Ma *et al.* 2019; Liu *et al.* 2020; Kuang *et al.* 2022; Madueke *et al.* 2022).

BC, a readily available and low-cost biomass-derived charcoal, can serve as a filler in PLA composites. Ho reported that increasing BC content enhanced the tensile strength of PLA, flexural strength, and ductility index by 43%, 99%, and 52%, respectively (Mitchell 1996). However, they also found that when the BC content exceeded 7.5 wt.%, its dispersion within the PLA matrix deteriorated, leading to poor interfacial bonding and compromised mechanical performance. Notably, deterioration at high filler loading is not governed solely by interfacial incompatibility (Ashraf *et al.* 2018). Particle agglomeration can form matrix-starved regions within clusters, resulting in weak load transfer and reduced tensile performance (Cionita *et al.* 2022). Therefore, uniform dispersion and sufficient melt infiltration are critical for maintaining mechanical integrity in BC/PLA composites with high BC content (Baniasadi *et al.* 2025). To overcome this dispersion challenge and maintain composite integrity, selecting an appropriate processing method is crucial (Nam *et al.* 2014; Patel *et al.* 2018; Mohammadi *et al.* 2022). Among various techniques, twin-screw extrusion pelletizing has gained widespread use in polymer composite fabrication due to its high production efficiency (Qian *et al.* 2018). Materials produced by this method exhibit improved mechanical properties. Moreover, its continuous processing capability helps reduce manufacturing costs. Therefore, although twin-screw extrusion shows great potential for producing BC/PLA composites with high filler content, the optimal processing parameters required to achieve uniform dispersion and strong interfacial bonding remain unclear.

This study aimed to develop highly filled BC-based degradable composites. Therefore, a series of BC/PLA composites were prepared using twin-screw extrusion, with a fixed PLA-to-BC mass ratio of 6:4 (w/w), which was determined through preliminary experiments to balance BC content and tensile performance. A three-factor, four-level orthogonal design was implemented, focusing on screw speed, temperature, and main feed rate to evaluate their effects on the composites' crystallization behavior, thermal behavior, and mechanical performance. This work systematically investigated the influence of key twin-screw extrusion processing parameters on the mechanical, thermal, and crystallization behaviors of BC/PLA composites at a fixed high BC loading of 40 wt.%, using an orthogonal experimental design.

EXPERIMENTAL

Sample Preparation

PLA FY601 had a density 1.24 of g/cm^3 and glass transition temperature of 60 ℃ (Anhui Fengyuan Biotechnology Co. Ltd). The BC powder (supplier-specified grade, carbonization temperature 800 °C), was provided by Shanghai Hainuo Carbon Co. In this study, the mass ratio of PLA to bamboo carbon (BC) was fixed at 6:4, corresponding to a BC content of 40 wt.% for all composite formulations, unless otherwise specified.

BC Physical and Chemical Properties Analysis

The BC powder was dried in an oven at 60 ℃ for 8 h. The standard and specimen samples were weighed by an electronic balance, with the mass of each sample being 50 to 60 mg. Disposable rubber gloves were put on during the weighing process, and wind blowing and vibration were avoided to prevent the measurement from being incorrect. The specimens and BC powder were wrapped with tinfoil and put into a carbon and nitrogen analyzer (G2131-I, Bicor, USA) for complete combustion, and the elemental content of BC powder was measured after calibrating the instrument with the specimens.

BC Particle Size Analysis

A certain amount of BC was placed in anhydrous ethanol and processed by ultrasonic shaking for 20 min. The particle size of BC was tested by laser particle sizer (MS 3000+EV, Malvern Panaco, UK), using deionized water as the dispersant with refractive index of dispersant of 1.33. The tabletop was kept tidy during the test to prevent any influence on the results.

Chemical Structure Analysis of BC

The chemical structure of BC was tested using a Fourier infrared spectrometer. A certain amount of BC powder and potassium bromide powder were distributed and wrapped in tinfoil and dried in an oven at 60 ℃ for 8 h. After drying, they were put into a mortar to be ground and mixed and pressed into thin slices, and the ratio of BC powder and potassium bromide was 1:100. The tests were performed under the following conditions: scanning range of 4000 to 400 cm^{-1}, instrumental resolution of 4 cm^{-1}, and the number of scans of the background and samples were both 32.

BC Specific Surface Area and Pore Analysis

The specific surface area and pore size of BC were analyzed using a fully automated specific surface area analyzer (ASAP 2460, McMurray Tick, USA). First, 100 mg of BC powder was placed in the instrument; the degassing temperature was set at 200 ℃ and the degassing time at 8 h for isothermal N_2 adsorption-desorption test. The specific surface area was calculated by the BET method, and the pore size distribution was derived from the BJH model.

Orthogonal Experimental Design and Preparation of BC/PLA Composites

A twin-screw extruder (Harbin Harp Electric Technology Co., Ltd.), which has a convenient speed of charging, good mixing ability, and good exhaust performance, is regarded as better than a single-screw extruder. That is because of its good processing performance, exhaust, and stability. Accordingly, twin-screw extruders are widely used in today's industrial production. Key parameters of the twin-screw extruder—such as screw

speed, screw type, processing temperature, and screw *L*/*D* ratio—have a significant effect on material transport and filler dispersion. Optimized settings promote uniform filler distribution, which is essential for maintaining the mechanical integrity of the composites (Rajeshkumar *et al.* 2021). The twin-screw extruder used in this study is shown in Fig. 1. Unless otherwise specified, all BC/PLA composites were prepared with a fixed PLA-to-BC mass ratio of 6:4 (corresponding to 40 wt.% BC). To investigate the optimum extrusion process for BC/PLA composites, Lg (34) orthogonal experiments were designed and analyzed with three factors, temperature (A), screw speed (B), and main feed speed (C) of the twin-screw extruder, based on preliminary processing trials conducted to determine feasible parameter ranges for stable extrusion. The orthogonal experimental factor levels are shown in Tables 2 2 and 2 3. BC and PLA were combined from the fourth zone of the twin-screw extruder, so the temperatures in the first to ninth zones of the twin-screw extruder were all set to 180, 185, 190, or 195 ℃ according to the orthogonal experimental design.

The BC and PLA were dried in an oven at 60 ℃ for 8 h. After drying, the BC was placed in the side feeding system of the twin-screw extruder, and the PLA was placed in the main feeding system, and the mass ratio of PLA to BC was 6:4. This PLA-to-BC ratio (6:4) was kept constant throughout all orthogonal experiments. The prepared BC/PLA composites were placed into a mold and made into sheets with a thickness of about 1 mm by using a flatbed vulcanizer. The temperature of the plate vulcanizing machine was 185 ℃, the pressure was 8 MPa, the first hot pressing time was 9 min, and the second hot pressing time was 5 min, the first hot pressing time needed to be manually pressurized in order to further remove air bubbles in the melt, and the molds were quickly put into the cold press and cooled down to room temperature after the hot pressing was completed. All composite sheets were prepared using identical hot-pressing parameters (185 °C and 8 MPa) to ensure consistent post-processing conditions. Therefore, the influence of hot pressing on the final properties was kept constant for all samples, and the observed differences can be primarily attributed to variations in extrusion processing parameters. Accordingly, the PLA-to-BC ratio of 6:4 was selected as the baseline composition for subsequent process optimization and property evaluation in this study.

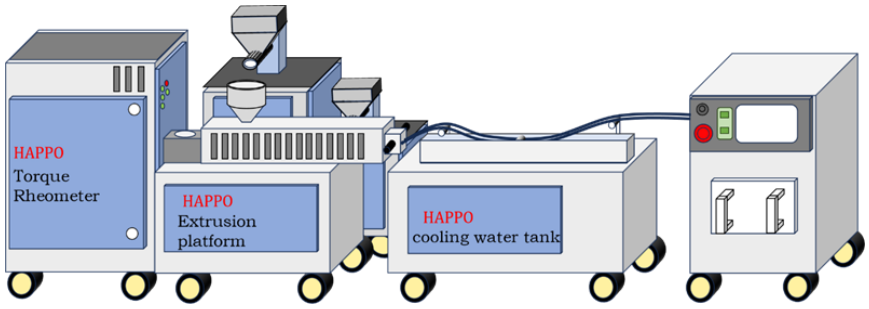

Fig. 1. Schematic diagram of twin-screw extruder

Table 1. Table of Factors and Levels for Orthogonal Experiments

	Factors		
	A (*T* °C)	B (Screw speed rpm/min)	C (Main feed flow rate g/min)
1	180	100	12.5
2	185	120	15
3	190	140	17.5
4	195	160	20

Table 2. Ability of Orthogonal Experiments

Samples	Factors		
	T (°C)	Screw speed (rpm/min)	Main feed flow rate (g/min)
BC-1	180	100	12.5
BC-2	180	120	15
BC-3	180	140	17.5
BC-4	180	160	20
BC-5	185	100	15
BC-6	185	120	12.5
BC-7	185	140	20
BC-8	185	160	17.5
BC-9	190	100	17.5
BC-10	190	120	20
BC-11	190	140	12.5
BC-12	190	160	15
BC-13	195	100	20
BC-14	195	120	17.5
BC-15	195	140	15
BC-16	195	160	12.5

Tensile Strength Test

The specimens were made and tested according to the national standard GB/T 1040.1 (2018). The sheets were cut into dumbbell-shaped specimens of 35 mm in length and 2 mm in width using a cutter (Fig. 2). The tensile properties of BC/PLA composites were tested using a microcomputer-controlled electronic universal testing machine (UTM2203, Shenzhen Sansi Zongheng Technology Co., Ltd.). The tensile rate was set to 1 mm/min. For each formulation, five specimens were tested under identical conditions, and the reported tensile strength represents the average value. No data were excluded from the analysis.

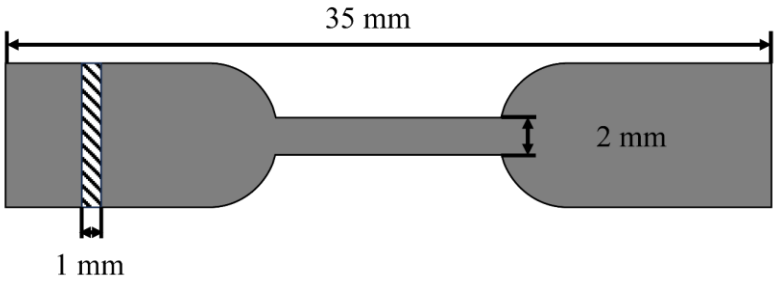

Fig. 2. Schematic diagram of the sample for the tensile test

X-ray Diffractometry

The BC/PLA composites were pulverized using a micro plant pulverizer (FT102, Tianjin Tester Instrument Co., Ltd.) and then sieved through a 200-mesh sieve to obtain the powder to be tested. The BC and BC/PLA composite powders and BC powders were tested by X-ray diffractometer. The X-ray diffractometer used a Cu target with a dwell time of 0.2 s per step, a step size of 0.02°, a 2θ range of 10° to 50°, an operating voltage of 40 kV, and an operating current of 40 mA.

Differential Scanning Calorimeter (DSC)

A differential scanning calorimeter (TA Q2000, Waters, USA) was used to test the thermal properties of BC/PLA composites. The composites were pulverized into powder using a pulverize and then about 10 mg of the sample was taken and sealed in the aluminum crucible of the instrument, and the test was carried out in a protective atmosphere of N_2. The sample was heated from 30 to 200 °C at a rate of 10 °C/min and kept at a constant temperature for 10 min to eliminate thermal history. The sample was then cooled to 30 °C at 10 °C/min and scanned by heating from 30 to 200 °C at 10 °C/min. The corresponding data of the second heating process was recorded. The degree of crystallinity (X_{CC}) was calculated as follows,

$$X_{CC}=\frac{\Delta H_m-\Delta H_{cc}}{\Delta H_0\times X_{PLA}}\times 100\% \quad (1)$$

where ΔH_m is the enthalpy of melting at the second warming of BC/PLA composites, ΔH_{cc} is the enthalpy of cold crystallization at the second warming of BC/PLA composites, and ΔH_0 is the enthalpy of 100% crystallization of PLA, *i.e.*, 93.6 J/g. X_{PLA} refers to the weight ratio of PLA in BC/PLA composites.

Thermogravimetric Analysis (TGA)

A thermogravimetric analyzer (TGA 4000, Perkin Elmer, USA) was used to analyze the heat loss characteristics of BC/PLA composites. A spray gun and alcohol were utilized to remove the impurities from the crucible, after which the clean crucible was placed on top of the tray inside the instrument, covered, and the researcher waited for the balance to be stable before zeroing. Once this was accomplished, the crucible was removed. Approximately 10 mg of sample was inserted and weighed by the instrument for testing. The instrument was heated at a rate of 10 °C/min over a temperature range of 30 to 500 °C with a protective gas of N_2 at a flow rate of 20 mL/min.

RESULTS AND DISCUSSION

Particle Size, Elemental Composition, Crystalline Structure, Chemical Structure, and Specific Surface Area of BC

Previous studies have demonstrated that an increase in pyrolysis temperature typically leads to a reduction in biochar yield as a result of intensified devolatilization, while simultaneously enhancing the degree of carbonization and structural ordering of the resulting bamboo carbon (Wang *et al.* 2024). However, higher pyrolysis temperatures promote a higher degree of carbonization, leading to increased fixed carbon content and more developed pore structures. As shown in Table 3, the carbon (C), hydrogen (H), and nitrogen (N) contents of BC were 96.2%, 0.57%, and 0.29%, respectively, indicating that elemental carbon is the primary component of BC. These results suggest that the BC powder was derived from high temperature pyrolyzed charcoal.

Table 3. Elemental Analysis of BC

Samples	C (%)	H (%)	N (%)
BC	96.22	0.57	0.29

The particle size distribution of BC is presented in Table 4. BC particles with smaller sizes possess higher surface energy and tend to agglomerate during composite preparation (Ramesh *et al.* 2021). In engineering applications, the D50 index is of primary concern. It represents the particle size at which 50% of the particles in the sample are smaller and 50% are larger. This value is commonly used to represent the median particle size of a powder sample. In this batch, 50% of the particles had diameters smaller than 6.32 μm, indicating a median particle size of 6.32 μm. The mesh designation provided by the supplier is regarded as a nominal commercial specification rather than a strict physical sieving criterion. The particle size of BC was characterized by laser diffraction, and the actual size distribution was evaluated based on D10, D50, and D90 values rather than nominal mesh size.

Table 4. Particle Size Distribution of BC

Samples	D_x(10) (μm)	D_x(50) (μm)	D_x(90) (μm)	D_x(97) (μm)	D_x(100) (μm)
BC	1.68	6.32	14.1	18.3	24.1

The crystalline structure of BC is illustrated in Fig. 3. High-temperature pyrolysis destroys the crystalline phase of cellulose, leading to its gradual degradation. As a result, the XRD pattern of BC powder exhibited broad diffraction peaks in the range of 15° to 30° and a distinct peak near 44°. These peaks correspond to the (100) plane (JCPDS 89-8487) and the (020) plane (JCPDS 74-2330) of the graphitic carbon structure (Liu *et al*. 2020).

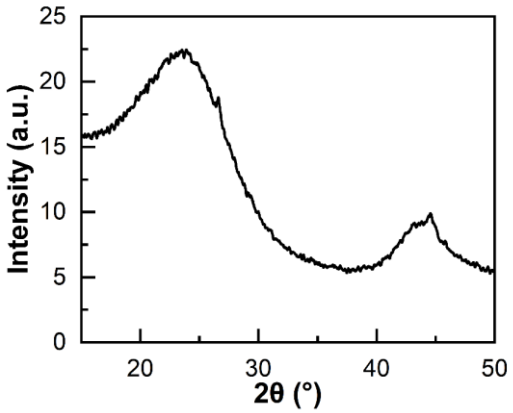

Fig. 3. Crystal structure of BC

An increased level of graphitization enhances not only the electron transfer capability and electrical conductivity of BC, but it also enhances its adsorption capacity and catalytic activity (Rasselet *et al.* 2014). Moreover, a higher degree of graphitization can stimulate microbial activity, thereby enhancing the anaerobic digestion of organic waste. BC produced via high-temperature pyrolysis exhibits good electrical conductivity, which must be addressed to mitigate potential interference in electromagnetic applications (Saravana *et al.* 2025).

Figure 4 shows the Fourier transform infrared (FTIR) spectra of BC, where the absorbance peaks around 3500 cm^{-1} indicate the presence of -OH groups on the surface of BC, and the absorbance peaks between 1527 cm^{-1} are due to the C=O stretching vibration of the COOH groups (Taib *et al.* 2023). This indicates that BC itself has a certain number of oxygen-containing groups.

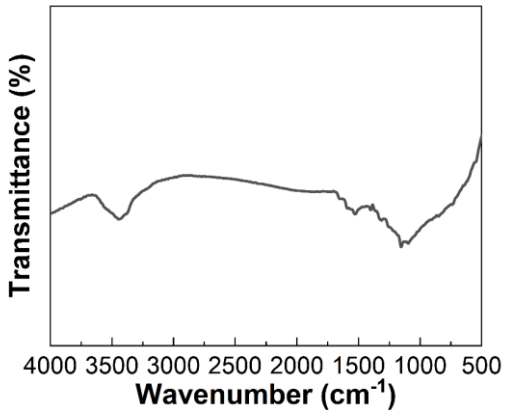

Fig. 4. FT-IR pattern of BC

The surface area, specific surface area, pore volume, and average pore diameter of the BC powder are summarized in Table 5. The BC powder exhibited a relatively high specific surface area, suggesting a larger contact interface with PLA and a greater potential for effective interfacial bonding. The average pore diameter reported in Table 5 was obtained from BJH analysis of the adsorption branch and corresponds to a volume-weighted average pore diameter rather than a number-based average. The isothermal nitrogen adsorption–desorption curve of BC is presented in Fig. 5a. The observed hysteresis (non-closure) of the adsorption–desorption curves can be attributed to the ink-bottle-shaped or non-rigid pore structures of BC. Such pores, characterized by narrow necks and wider bodies, impede complete nitrogen desorption, resulting in a desorption branch that lies above the adsorption curve. As shown in Fig. 5b, most of pores in the BC sample were concentrated in the 3 to 4 nm range.

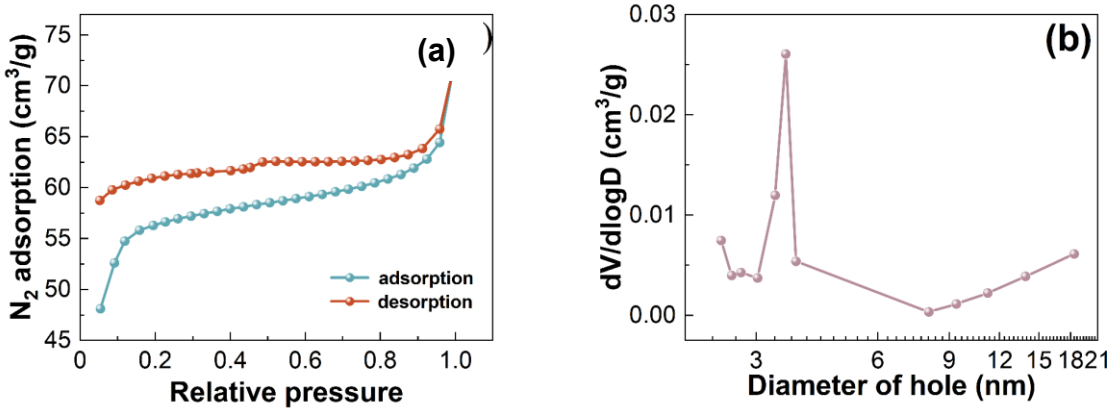

Fig. 5. N_2 adsorption–desorption isotherms (a) and pore size distribution (b) of BC

Table 5. Porous Properties of BC Determined from N_2 Adsorption–desorption

Samples	Surface area (m^2/g)	Specific surface area (m^2/g)	Pore volume (cm^3/g)	Average pore diameter (nm)
BC	197.99	187.81	0.083	2.23

Effect of Process Parameters on Tensile Properties of BC/PLA Composites

The range analysis of tensile strength based on the orthogonal tests is presented in Table 6. The R values for temperature, screw speed, and main feed flow rate were 11.97, 9.08, and 6.06, respectively. Therefore, the order of influence on the tensile strength of the BC/PLA composites was temperature > screw speed > main feed flow rate. Temperature directly affects the melting behavior of the PLA matrix (Wang *et al*. 2018; Trivedi *et al*. 2023). If the temperature is too low, the PLA matrix does not melt sufficiently, making it difficult to disperse the BC filler uniformly, which can lead to stress concentrations. Conversely, excessively high temperatures can cause thermal degradation of the PLA matrix, break molecular chains, and further reduce its mechanical properties (Wang *et al*. 2020; Wang *et al*. 2021). High screw speeds generate strong shear forces that enhance PLA flow into BC pores and promote filler dispersion. However, as with high temperatures, excessive screw speed can hinder adequate bonding between PLA and BC, reduce cross-linking, and degrade the matrix mechanically, ultimately lowering tensile strength. An excessively high main feed flow rate may result in barrel overfilling and increased torque, which could trigger the extruder's safety mechanisms or even causing mechanical failure. Before mixing, it is essential to dry the raw materials, as the filler can absorb ambient moisture, which evaporates under high extrusion temperatures, forming internal bubbles that compromise filler–matrix adhesion and overall composite performance.

In materials science, the range-analysis method provides significant advantages, allowing rapid determination of the critical parameters governing system response and their optimal settings. By assessing the magnitude of factor-level effects on response variables, this method rapidly identifies the key factors governing material properties. Quantitative comparison of extreme values enables the identification of primary and secondary factors, as well as their interactions, that affect material performance. Applying this method to the processing optimization of BC/PLA composites allows for the effective determination of optimal twin-screw extrusion parameters.

As shown in Table 6, the extreme difference values followed the order $R_A > R_B > R_C$, indicating that the influence of factors ranked as: temperature > screw speed > main feed flow rate. Among the three factors, the highest R-values were k_4, k_2, and k_2, respectively. Thus, the optimal processing combination was temperature 195 °C, screw speed 120 rpm, and main feed flow rate 15 g/min. The tensile strength of the BC/PLA composites prepared under this condition reached 40.86 MPa, outperforming all other process conditions. Thus, this process combination enhanced the composite's tensile strength.

Additionally, the tensile strengths of BC-9 and BC-11 were significantly lower than those of other samples. The extremely low tensile strengths observed for BC-9 and BC-11 were reproducible across repeated tests and were therefore not treated as outliers. No data elimination was performed. These low values reflect unstable extrusion conditions that led to poor BC dispersion and weak interfacial bonding. For BC-9 (190 °C, 100 rpm, 17.5 $g \cdot min^{-1}$), the relatively low screw speed combined with a high feed rate likely resulted in insufficient shear stress, leading to poor BC dispersion and local agglomeration within the PLA matrix. In contrast, BC-11 (190 °C, 140 rpm, 12.5 $g \cdot min^{-1}$) experienced excessive shear relative to the feeding rate, which may have caused PLA chain degradation and unstable melt flow. Both parameter combinations fell outside the stable processing window, resulting in weak interfacial bonding and significantly reduced tensile strength. This mismatch may have impaired the BC–PLA interfacial bonding and caused severe BC agglomeration, ultimately reducing the composite's tensile strength.

Table 6. Results of Orthogonal Experiments

Samples	*T* (°C)	Screw Speed (rpm/min)	Main Feed Flow Rate (g/min)	Tensile Strength (MPa)
BC-1	180	100	12.5	29.67
BC-2	180	120	15	30.43
BC-3	180	140	17.5	24.95
BC-4	180	160	20	31.19
BC-5	185	100	15	32.17
BC-6	185	120	12.5	36.31
BC-7	185	140	20	22.4
BC-8	185	160	17.5	32.56
BC-9	190	100	17.5	8.5
BC-10	190	120	20	31.5
BC-11	190	140	12.5	12.12
BC-12	190	160	15	25.21
BC-13	195	100	20	30.3
BC-14	195	120	17.5	31.47
BC-15	195	140	15	33.92
BC-16	195	160	12.5	29.51
k1	29.06	25.16	26.90	-
k2	30.86	32.43	30.43	-
k3	19.33	23.35	24.37	-
k4	31.30	29.62	28.85	-
R	11.97	9.08	6.06	-
Order of influence	T＞Screw speed＞Main feed flow rate			

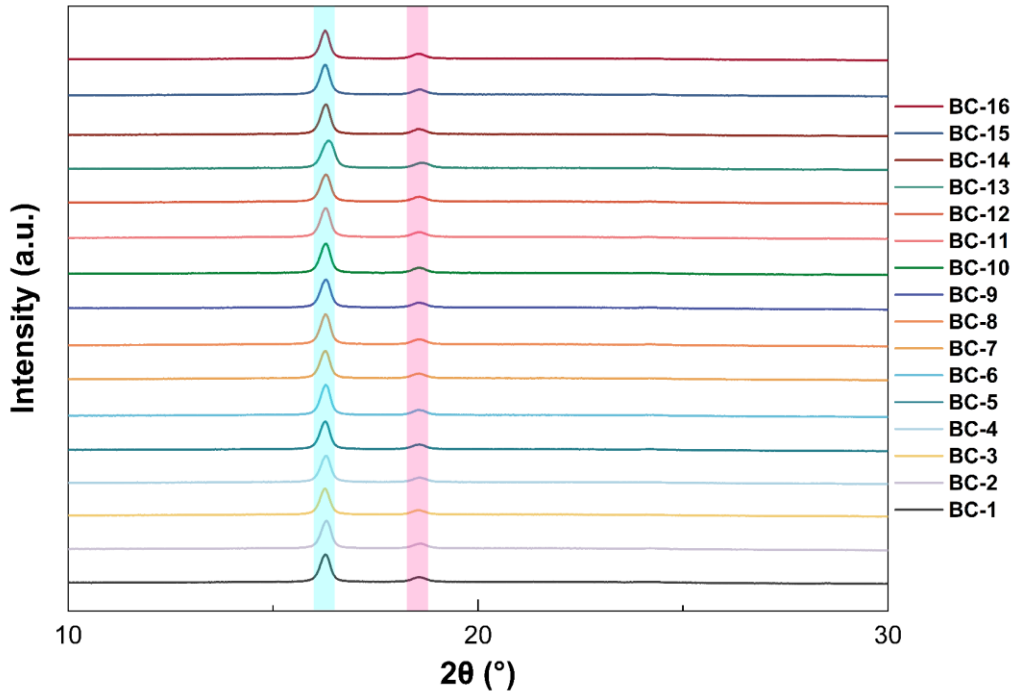

Fig. 6. Effect of different process parameters on the crystal structure of BC/PLA composites

Effect of Process Parameters on the Crystalline Structure of BC/PLA Composites

Figure 6 illustrates the influence of various processing parameters on the X-ray diffraction (XRD) patterns of BC/PLA composites. Despite the different processing conditions, all samples exhibited similar characteristic diffraction peaks at approximately 16° and 18°, corresponding to the (200)/ (100) and (203) crystal planes, respectively. The crystalline structure of the BC/PLA composites remained unchanged under different processing conditions. The peak intensities and widths were comparable across all samples, and the PLA crystalline form remained predominant. Minor shifts in peak positions to the left or right were observed depending on the processing parameters, however, these shifts were not substantial. Overall, the processing parameters had no significant effect on the crystalline structure of PLA.

Influence of Process Parameters on Thermal Properties of BC/PLA Composites

Figure 7 illustrates the effects of various processing parameters on the second heating curve obtained from the differential scanning calorimetry (DSC) analysis of the BC/PLA composites.

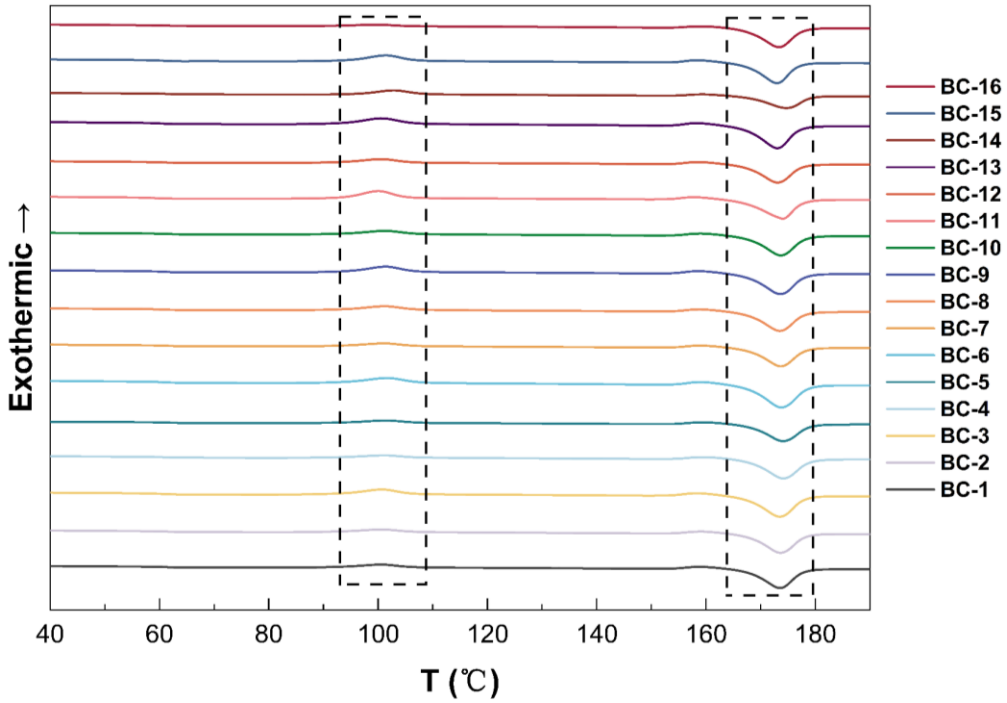

Fig. 7. DSC secondary heating curves of BC/PLA composites with different process parameters

Table 7 summarizes the thermal parameters for each composite group. As shown in the graphs, the glass transition temperature (T_g), cold crystallization temperature (T_c), and melting temperature (T_m) exhibited minimal variation across different processing conditions, whereas the enthalpy of cold crystallization (ΔH_{cc}) and the melting enthalpy (ΔH_m) varied noticeably. All samples exhibited a crystallization peak near 100 °C and a melting peak around 173 °C. The crystalline of the samples ranged from 47% to 57%, which can be attributed to variations in extrusion conditions affecting the dispersion of BC

within the PLA matrix. This, in turn, influenced the crystallization behavior of PLA and ultimately affected the overall crystallinity of the composites. While the different processing parameters had little effect on T_g, T_c, and T_m, they did influence ΔH_{cc} and ΔH_m to some extent.

Table 7. Thermal Characteristic Parameters of BC/PLA Composites with Different Process Parameters

Samples	T_g (°C)	T_c (°C)	T_m (°C)	ΔH_{cc} (J/g)	ΔH_m (J/g)	X_c (%)
BC-1	61.36	100.52	173.42	8.82	37.97	51.90
BC-2	61.60	100.96	173.51	7.78	38.18	54.13
BC-3	61.14	100.66	173.54	12.35	39.85	48.97
BC-4	61.58	101.25	174.04	7.34	36.39	51.72
BC-5	60.96	101.62	173.93	7.70	36.16	50.68
BC-6	61.96	101.71	173.70	11.61	40.41	51.28
BC-7	62.00	101.09	173.55	8.47	38.18	52.91
BC-8	61.63	101.26	173.37	11.23	39.16	49.73
BC-9	61.36	101.53	173.38	12.61	39.18	47.31
BC-10	61.96	101.71	173.70	11.61	40.41	51.28
BC-11	59.60	100.07	173.90	16.36	41.86	45.41
BC-12	60.57	100.67	172.98	10.17	38.21	49.93
BC-13	61.41	100.46	172.92	13.84	41.03	48.42
BC-14	60.61	97.71	173.72	2.91	31.57	51.03
BC-15	61.01	101.51	172.88	13.95	41.11	48.36
BC-16	61.21	100.26	173.30	4.35	36.10	56.54

The variations in ΔH_{cc} and ΔH_m can be attributed to differences in BC dispersion and the resulting mobility of PLA molecular chains induced by processing parameters. Under appropriate temperature and screw speed conditions, well-dispersed BC particles can act as heterogeneous nucleation sites, facilitating PLA crystallization during heating and leading to higher ΔH_m and lower ΔH_{cc} (Haeldermans *et al.* 2021). This enhanced crystallization behavior is generally associated with improved tensile performance, as a more developed crystalline structure contributes to higher load-bearing capability.

In contrast, insufficient or excessive shear during extrusion may lead to BC agglomeration or PLA chain degradation, which restricts chain rearrangement and crystallization, resulting in increased ΔH_{cc} and reduced effective crystallinity (Mysiukiewicz *et al.* 2020). This trend is consistent with the lower tensile strengths observed for samples processed outside the optimal parameter window.

Effect of Process Parameters on Thermal Stability of BC/PLA Composites

As shown in Fig. 8 and Table 8, the mass loss curves of the BC/PLA composites containing 40 wt.% BC (PLA:BC = 6:4), prepared under different processing parameters exhibited similar thermal degradation behavior, with only slight variations. Notably, the BC-1 sample exhibited a slightly lower onset decomposition temperature compared to the others. Overall, all samples demonstrated minimal mass loss below 250 °C, which can be primarily attributed to the evaporation of absorbed moisture, as BC is prone to hygroscopicity (Xie *et al*. 2010; Wu *et al*. 2022). This minor weight loss did not significantly affect the structural integrity of the composites, indicating that th e BC/PLA materials possessed good thermal stability within typical service temperature ranges. Upon reaching approximately 250 °C, all samples began to undergo pyrolysis, indicating the initiation of PLA molecular chain scission. The onset decomposition

temperature ($T_{5\%}$) for most samples was around 300 °C, with BC-1 being a slight exception, suggesting that processing conditions had limited influence on the thermal stability of the composites. Figure 9 further shows the mass loss rate of the same BC/PLA composites containing 40 wt.% BC under different processing conditions. The differential thermogravimetric (DTG) curves presented in Fig. 9 demonstrate that all samples exhibited a sharp, single degradation peak, with maximum weight loss rates occurring around 330 °C, ranging between 17%/min and 20%/min. This consistent single-peak pattern indicates a rapid and concentrated degradation process common across all samples, reinforcing the conclusion that varying the processing parameters did not significantly affect thermal decomposition characteristics. At the final analysis temperature of 500 °C, the residual carbon content remained within the 35 to 40% range across all samples. The relatively low mass retention could be attributed to partial BC loss during extrusion. Specifically, due to its moisture-absorbing nature, some BC may have adhered to the inner wall of the feeder and failed to enter the twin-screw extruder, potentially due to bridging. Consequently, the PLA melt might not have fully interacted with the BC before exiting the extrusion zone, resulting in reduced BC content in some samples. In summary, while minor variations in BC content may occur due to processing limitations, the BC/PLA composites prepared under different processing parameters consistently exhibited good thermal stability and comparable degradation characteristics.

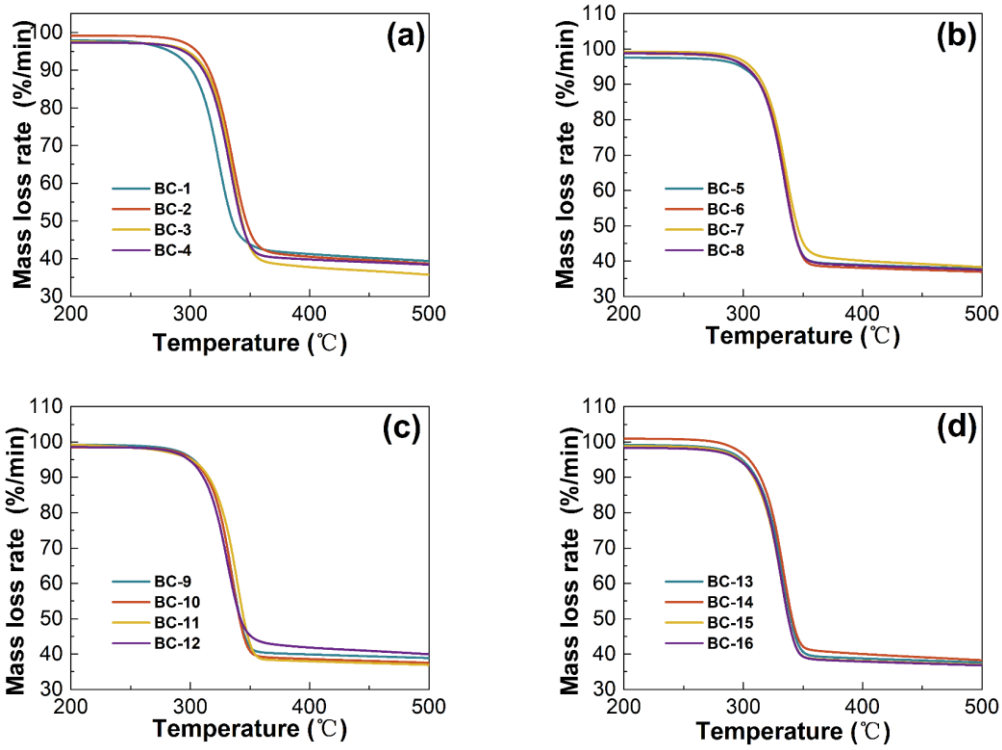

Fig. 8. Effect of different process parameters on thermal stability of BC/PLA composites containing 40 wt.% BC (PLA:BC = 6:4). (a) Samples numbered BC-1 to 4; (b) Samples numbered BC-5 to 8; (c) Samples numbered BC-9 to 12 (d) Samples numbered BC13-16

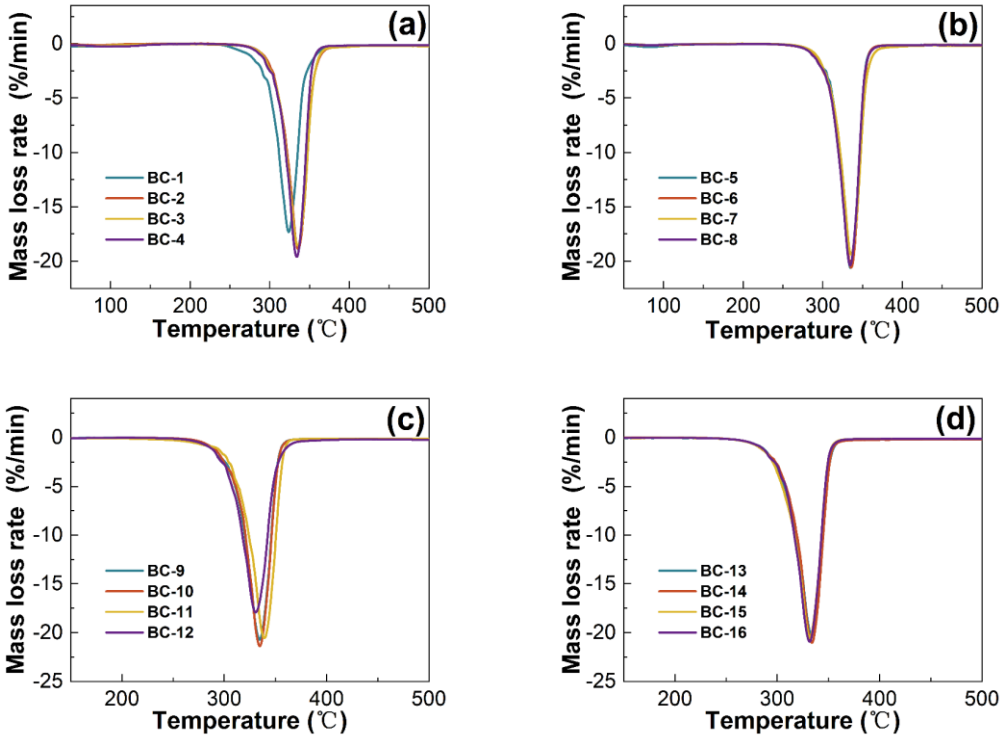

Fig. 9. Effect of different process parameters on mass loss rate of BC/PLA composites containing 40 wt.% BC (PLA:BC = 6:4). (a) samples numbered BC-1 to BC-4; (b) samples numbered BC-5 to BC-8; (c) samples numbered BC-9 to BC-12; (d) samples numbered BC-13 to BC-16

Table 8. TGA Results of BC/PLA Composites Prepared by Different Process Parameters

Samples	$T_{-5\%}$ (°C)	R_{peak} (%/min)/ T_{max} (°C)	Mass loss (%)
BC-1	282.97	17.31/323.58	39.40
BC-2	305.53	18.88/335.63	38.68
BC-3	297.85	18.564/335.37	35.77
BC-4	294.64	19.59/333.72	38.44
BC-5	298.34	20.61/334.77	37.82
BC-6	301.89	20.58/335.46	36.95
BC-7	306.17	19.39/335.54	38.29
BC-8	301.43	20.38/334.30	37.53
BC-9	302.63	20.72/334.45	38.88
BC-10	301.26	21.37/334.61	37.54
BC-11	300.73	20.56/338.95	36.94
BC-12	298.71	17.91/330.33	39.97
BC-13	298.86	20.17/332.96	37.62
BC-14	304.86	21.03/333.6	38.26
BC-15	296.92	20.53/331.84	36.98
BC-16	295.74	20.91/331.58	36.81

Analysis of Tensile Properties of BC/PLA Composites

Figure 10 shows the effect of BC addition on the tensile strength of BC/PLA composites. The experimental results showed that the tensile strength of pure PLA was 37.4 MPa, while Van der Waals forces were formed between BC and PLA matrix, which

in turn enhanced the tensile strength of the composites (Ye *et al*. 2019; Zhu and Wang 2024). To further validate the rationality of the selected PLA-to-BC ratio (6:4), composites with different BC contents were prepared under identical processing conditions for comparison. This comparison was intended to demonstrate the relative advantages of the 6:4 ratio in terms of tensile performance while considering BC utilization, rather than to re-optimize the composition. It was found that the tensile strength of PLA was still higher than that of pure PLA when the ratio of PLA to BC was 6:4, and the tensile strength was found to be significantly lower than the tensile strength of pure PLA when BC was added up to half again.

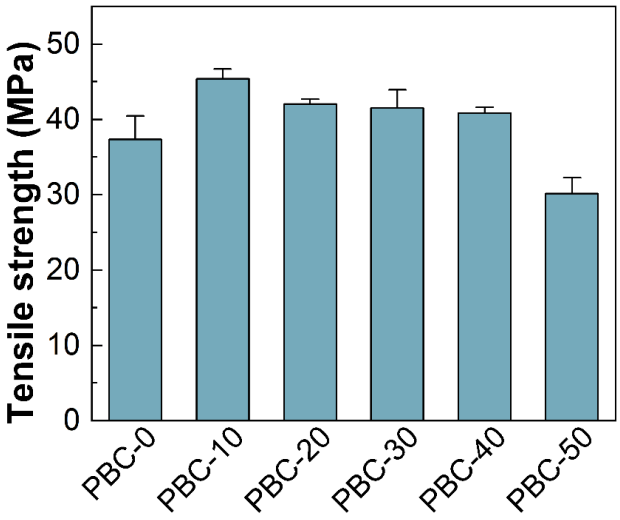

Fig. 10. Tensile properties of BC/PLA composites

In this study, an L16(4^3) orthogonal experimental design was employed to investigate the effects of three key processing parameters—temperature, screw speed, and main feed flow rate—on the crystalline structure, thermal properties, and mechanical performance of BC/PLA composites using twin-screw extrusion. The results showed that variations in these processing conditions had limited influence on the crystalline structure, thermal stability, and thermal transitions of the composites. The X-ray diffraction patterns of all samples exhibited two characteristic peaks around 16° and 18°, corresponding to the (200/100) and (203) crystalline planes of PLA, respectively, indicating no significant structural changes. Most composites exhibited similar onset decomposition temperatures and residual mass retention rates between 35% and 40%. Slightly lower mass retention observed in a few samples was attributed to a "bridging" phenomenon during extrusion, which led to incomplete BC feeding. The glass transition temperature (T_g), cold crystallization temperature (T_{cc}), and melting temperature (T_m) of all composites were also consistent, occurring at approximately 60, 100, and 173 °C, respectively. However, differences in BC dispersion caused slight variations in crystallinity among the samples. The range analysis of tensile strength revealed that temperature had the most significant effect, followed by screw speed and main feed flow rate. Based on the orthogonal test results, the optimal processing parameters were identified as an extrusion temperature of 195 °C, a screw speed of 120 rpm, and a feed rate of 15 g/min. This study provides a foundation for further process optimization and material modification of BC/PLA composites. Based on the above comparison, the PLA-to-BC ratio of 6:4 shows a favorable balance between tensile performance and BC content.

CONCLUSIONS

1. The effects of different processing techniques on the crystalline structure, thermal stability, and thermal properties of the BC/PLA composites were not significant.
2. The optimal processing parameters for BC/PLA composites were determined through orthogonal testing as follows: an extrusion temperature of 195 °C, a screw speed of 120 rpm, and a main feed flow rate of 15 g/min.
3. To reduce the cost of fully bio-based composites while maintaining sufficient mechanical strength, the PLA-to-BC ratio of 6:4 showed a favorable balance between tensile performance and BC content under the investigated processing conditions.

ACKNOWLEDGMENTS

This work was carried out with the financial support of the National Key Research and Development Program of China (Grant number: 2023YFD220210401) and the Research and Demonstration of Key Technologies for "Bamboo as Substitute for Plastic" in Pilot Member States of the International Bamboo and Rattan Organization (INBAR) "New Value- added Technology of Full Utilizing Small-diameter Bamboo as Substitute for Plastic" (23-1396-2023091101).

Credit Authorship Contribution Statement

HaoXiang Fang: Original draft, Software, Investigation, Formal analysis, Conceptualization. YuXuan Chen: Supervision, Methodology. LinPeng Yu: Methodology, Investigation. KangJian Zhang: Methodology, Data curation. Ping Zhu: Data curation. Bin Xu: Resources, Supervision. Genlin Tian: Project administration, Funding acquisition.

Declaration of Competing Interest

The authors declare that they have no known competing financial interests or personal relationships that could have appeared to influence the work reported in this paper.

Data Availability

Data will be made available on request.

REFERENCES CITED

Alarifi, I. M. (2023). "A review on factors affecting machinability and properties of fiber-reinforced polymer composites," *Journal of Natural Fibers* 20(1), article 2154304. https://doi.org/10.1080/15440478.2022.2154304

Anwer, M. A. S., and Naguib, H. E. (2016). "Study on the morphological, dynamic mechanical and thermal properties of PLA carbon nanofibre composites," *Composites Part B: Engineering* 91, 631-639. https://doi.org/10.1016/j.compositesb.2016.01.039

Ashraf, M. A., Peng, W., Zare, Y., and Rhee, K. Y. (2018). "Effects of size and aggregation/agglomeration of nanoparticles on the interfacial/interphase properties and tensile strength of polymer nanocomposites," *Nanoscale Research Letters* 13, article 214. https://doi.org/10.1186/s11671-018-2624-0

Backes, E. H., Pires, L. N., Costa, L. C., Passador, F. R., and Pessan, L. A. (2019). "Analysis of the degradation during melt processing of PLA/Biosilicate® composites," *Journal of Composites Science* 3(2), article 52. https://doi.org/10.3390/jcs3020052

Baniasadi, H., Puttonen, T., Abidnejad, R., Jayaprakash, S., Partanen, J., Lizundia, E., and Niskanen, J. (2025). "Biochar-reinforced polyamide 12 composites for sustainable selective laser sintering 3D printing: Performance enhancement and carbon footprint reduction," *Chemical Engineering Journal* 519, 165502. https://doi.org/10.1016/j.cej.2025.165502

Binner, J., Porter, M., Baker, B., Zou, J., Venkatachalam, V., Diaz, V. R., D'Angio, A., Ramanujam, P., Zhang, T., and Murthy, T. (2020). "Selection, processing, properties and applications of ultra-high temperature ceramic matrix composites, UHTCMCs – A review," *International Materials Reviews* 65(7), 389-444. https://doi.org/10.1080/09506608.2019.1652006

Chaudhary, B., Thoi, H. H., Karande, S., Kao, C. I., Terbrueggen, R. H., Babb, D. A., Cummins, C. H., Mullins, M. J., and Silvis, C. H. (2001). "Crosslinking of polymers and foams thereof," U.S. Patent No. 6325956B2.

Cionita, T., Siregar, J. P., Shing, W. L., Hee, C. W., Fitriyana, D. F., Jaafar, J., Junid, R., Irawan, A. P., and Hadi, A. E. (2022). "The influence of filler loading and alkaline treatment on the mechanical properties of palm kernel cake filler reinforced epoxy composites," *Polymers* 14(15), article 3063. https://doi.org/10.3390/polym14153063

Cuadri, A., and Martín-Alfonso, J. (2018). "Thermal, thermo-oxidative and thermo-mechanical degradation of PLA: A comparative study based on rheological, chemical and thermal properties," *Polymer Degradation and Stability* 15, 37-45. https://doi.org/10.1016/j.polymdegradstab.2018.02.011

Dobrzański, L. A. (2006). "Significance of materials science for the future development of societies," *Journal of Materials Processing Technology* 175(1-3), 133-148. https://doi.org/10.1016/j.jmatprotec.2005.04.003

Douglas, J., Gardner, Y., Han, L., and Wang, Y. (2015). "Wood–plastic composite technology," *Current Forestry Reports* 1(3), 139-150. https://doi.org/10.1007/s40725-015-0016-6

Dubey, S. P., Thakur, V. K., Krishnaswamy, S., Abhyankar, H. A., Marchante, V., and Brighton, J. L. (2017). "Progress in environmental-friendly polymer nanocomposite material from PLA: Synthesis, processing and applications," *Vacuum* 146, 655-663. https://doi.org/10.1016/j.vacuum.2017.07.009

Ferdinand, M., Várdai, R., Móczó, J., and Pukanszky, B. (2023). "A novel approach to the impact modification of PLA," *Engineering Fracture Mechanics* 277, article 108950. https://doi.org/10.1016/j.engfracmech.2022.108950

Friedrich, K., and Almajid, A. A. (2013). "Manufacturing aspects of advanced polymer composites for automotive applications," *Applied Composite Materials* 20(2), 107-128. https://doi.org/10.1007/s10443-012-9258-7

Fu, S.-Y., Feng, X.-Q., Lauke, B., and Mai, Y.-W. (2008). "Effects of particle size, particle/matrix interface adhesion and particle loading on mechanical properties of particulate–polymer composites," *Composites Part B: Engineering* 39(6), 933-961. https://doi.org/10.1016/j.compositesb.2008.01.002

GB/T 1040.1 (2018). "Plastics – Determination of tensile properties - Part 1: General principles," Standardization Administration of China, Beijing.

Ghorbani, M., and Amirahmadi, E. (2024). "Insights into soil and biochar variations and

their contribution to soil aggregate status – A meta-analysis," *Soil and Tillage Research* 244, article 106282. https://doi.org/10.1016/j.still.2024.106282

Haeldermans, T., Samyn, P., Cardinaels, R., Vandamme, D., Vanreppelen, K., Cuypers, A., Schreurs, S. (2021). "Poly (lactic acid) biocomposites containing biochar particles: effects of fillers and plasticizers on crystallization and thermal properties," *Express Polymer Letters* 15, 343-360. https://doi.org/10.3144/expresspolymlett.2021.30

Hietala, M., and Oksman, K. (2018). "Pelletized cellulose fibres used in twin-screw extrusion for biocomposite manufacturing: Fibre breakage and dispersion," *Composites Part A: Applied Science and Manufacturing* 109, 538-545. https://doi.org/10.1016/j.compositesa.2018.04.006

Ho, M.-P., Lau, K.-T., Wang, H., and Hui, D. (2015). "Improvement on the properties of polylactic acid (PLA) using bamboo charcoal particles," *Composites Part B: Engineering* 81, 14-25. https://doi.org/10.1016/j.compositesb.2015.05.048

Kuan, C.-F., Kuan, H.-C., Ma, C.-C. M., and Chen, C.-H. (2008). "Mechanical and electrical properties of multi-wall carbon nanotube/poly(lactic acid) composites," *Journal of Physics and Chemistry of Solids* 69(5-6), 1395-1398. https://doi.org/10.1016/j.jpcs.2007.10.060

Kuang, T., Esmaeili, A., and Ehsani, M. (2022). "Eco-friendly biodegradable polymers: Sustainable future," *Polymers from Renewable Resources* 13(1-2), 71-79. https://doi.org/10.1177/20412479221109875

Liu, H., and Zhang, J. (2011). "Research progress in toughening modification of poly(lactic acid)," *Journal of Polymer Science Part B: Polymer Physics* 49(15), 1051-1083. https://doi.org/10.1002/polb.22283

Liu, J., Zhang, Q.-H., Ma, F., Zhang, S.-F., Zhou, Q., and Huang, A.-M. (2020). "Three-step identification of infrared spectra of similar tree species to *Pterocarpus santalinus* covered with beeswax," *Journal of Molecular Structure* 1218, article 128484. https://doi.org/10.1016/j.molstruc.2020.128484

Ma, Y., Qian, S., Hu, L., Qian, J., Fontanillo Lopez, C. A., and Xu, L. (2019). "Mechanical, thermal, and morphological properties of PLA biocomposites toughened with silylated bamboo cellulose nanowhiskers," *Polymer Composites* 40(8), 3012-3019. https://doi.org/10.1002/pc.25144

Madueke, C. I., Umunakwe, R., and Mbah, O. M. (2022). "A review on the factors affecting the properties of natural fibre polymer composites," *Nigerian Journal of Technology* 41(1), 55-64. https://doi.org/10.4314/njt.v41i1.9

Mitchell, P. E. (1996). *Plastic Part Manufacturing*, Society of Manufacturing Engineers.

Mohammadi, H., Ahmad, Z., Mazlan, S. A., Faizal Johari, M. A., Siebert, G., Petrů, M., and Rahimian Koloor, S. S. (2022). "Lightweight glass fiber-reinforced polymer composite for automotive bumper applications: A review," *Polymers* 15(1), article 193. https://doi.org/10.3390/polym15010193

Mysiukiewicz, O., Barczewski, M., Skórczewska, K., Matykiewicz, D. (2020). "Correlation between processing parameters and degradation of different polylactide grades during twin-screw extrusion," *Polymers* 12, article 1333.

Nam, D. H., Kim, J. H., Cha, S. I., Jung, S. I., Lee, J. K., Park, H. M., Park, H. D., and Hong, S. H. (2014). "Hardness and wear resistance of carbon nanotube reinforced aluminum-copper matrix composites," *Journal of Nanoscience & Nanotechnology* 14(12), 9134-9138. https://doi.org/10.1166/jnn.2014.10084

Patel, M., Pardhi, B., Chopara, S., and Pal, M. (2018). "Lightweight composite materials

for automotive – A review," *Carbon* 1(2500), article 151.
Qian, S., Zhang, H., Yao, W., and Sheng, K. (2018). "Effects of bamboo cellulose nanowhisker content on the morphology, crystallization, mechanical, and thermal properties of PLA matrix biocomposites," *Composites Part B: Engineering* 133, 203-209. https://doi.org/10.1016/j.compositesb.2017.09.040
Rajeshkumar, G., Seshadri, S. A., Devnani, G., Sanjay, M., Siengchin, S., Maran, J. P., Al-Dhabi, N. A., Karuppiah, P., Mariadhas, V. A., and Sivarajasekar, N. (2021). "Environment friendly, renewable and sustainable poly lactic acid (PLA) based natural fiber reinforced composites – A comprehensive review," *Journal of Cleaner Production* 310, article 127483. https://doi.org/10.1016/j.jclepro.2021.127483
Ramesh, M., Rajeshkumar, L., and Balaji, D. (2021). "Influence of process parameters on the properties of additively manufactured fiber-reinforced polymer composite materials: A review," *Journal of Materials Engineering and Performance* 30(7), 4792-4807. https://doi.org/10.1007/s11665-021-05832-y
Rasselet, D., Ruellan, A., Guinault, A., Miquelard-Garnier, G., Sollogoub, C., and Fayolle, B. (2014). "Oxidative degradation of polylactide (PLA) and its effects on physical and mechanical properties," *European Polymer Journal* 50, 109-116. https://doi.org/10.1016/j.eurpolymj.2013.10.011
Saravana Kumar, M., Yang, C. H., Vignesh, M., Edoziuno, F. O., Romanovski, V., and Salah, B. (2025). "Optimizing the filler distribution to enhance the interlaminar shear strength and impact resistance of fiber reinforced epoxy composites," *Polymer Composites* 46(14), 12650-12662. https://doi.org/10.1002/pc.29885
Taib, N.-A. A. B., Rahman, M. R., Huda, D., Kuok, K. K., Hamdan, S., Bakri, M. K. B., Julaihi, M. R. M. B., and Khan, A. (2023). "A review on poly lactic acid (PLA) as a biodegradable polymer," *Polymer Bulletin* 80(2), 1179-1213. https://doi.org/10.1007/s00289-022-04160-y
Trivedi, A. K., Gupta, M., and Singh, H. (2023). "PLA based biocomposites for sustainable products: A review," *Advanced Industrial and Engineering Polymer Research* 6(4), 382-395. https://doi.org/10.1016/j.aiepr.2023.02.002
Wang, F., Zhou, S., Yang, M., Chen, Z., and Ran, S. (2018). "Thermo-mechanical performance of polylactide composites reinforced with alkali-treated bamboo fibers," *Polymers* 10(4), article 401. https://doi.org/10.3390/polym10040401
Wang, J., Li, Z., Li, Y., Wang, Z., Liu, X., Liu, Z., and Ma, J. (2024). "Evolution and correlation of the physiochemical properties of bamboo char under successive pyrolysis process," *Biochar* 6, article 321. https://doi.org/10.1007/s42773-024-00321-6
Wang, M., Chen, Y., Fu, H., Qu, X., Li, B., Tao, S., and Zhu, D. (2020). "An investigation on hygroscopic properties of 15 black carbon (BC)-containing particles from different carbon sources: Roles of organic and inorganic components," *Atmospheric Chemistry and Physics* 20(13), 7941-7954. https://doi.org/10.5194/acp-20-7941-2020
Wang, M., Chen, Y., Fu, H., Qu, X., Shen, G., Li, B., and Zhu, D. (2021). "Combined analyses of hygroscopic properties of organic and inorganic components of three representative black carbon samples recovered from pyrolysis," *Science of The Total Environment* 771, article 145393. https://doi.org/10.1016/j.scitotenv.2021.145393
Wu, F., Xie, J., Xin, X., and He, J. (2022). "Effect of activated carbon/graphite on enhancing anaerobic digestion of waste activated sludge," *Frontiers in Microbiology* 13, article 999647. https://doi.org/10.3389/fmicb.2022.999647
Xie, Z., Liu, Z., Wang, Y., Yang, Q., Xu, L., and Ding, W. (2010). "An overview of

recent development in composite catalysts from porous materials for various reactions and processes," *International Journal of Molecular Sciences* 11(5), 2152-2187. https://doi.org/10.3390/ijms11052152

Ye, S., Yan, M., Tan, X., Liang, J., Zeng, G., Wu, H., Song, B., Zhou, C., Yang, Y., and Wang, H. (2019). "Facile assembled biochar-based nanocomposite with improved graphitization for efficient photocatalytic activity driven by visible light," *Applied Catalysis B: Environmental* 250, 78-88. https://doi.org/10.1016/j.apcatb.2019.03.004

Zhu, T., and Wang, Z. (2024). "Advances in processing and ablation properties of carbon fiber reinforced ultra-high temperature ceramic composites," *Reviews on Advanced Materials Science* 63(1), article 20240029. https://doi.org/10.1515/rams-2024-0029

Article submitted: October 1, 2025; Peer review completed: January 17, 2026; Revised version received and accepted: February 8, 2026; Published: February 24, 2026.
DOI: 10.15376/biores.21.2.3449-3468